A Mixed Lewis Acid-Brønsted Acid Ambient Temperature Ionic Liquid: An Electrochemical and NMR Study of Dimethylaniline

Soo-Gil Park,† Paul C. Trulove, Richard T. Carlin,‡ and Robert A. Osteryoung*

Contribution from the Department of Chemistry, State University of New York, Buffalo, New York 14214. *Received August 16, 1990. Revised Manuscript Received January 11, 1991*

Abstract: A mixed Lewis-Brønsted acid ambient temperature chloroaluminate molten salt, in which both the Lewis and Brønsted acidity may be varied, has been investigated making use of a probe solute molecule. The interaction of the proton and molten salt solvent with *N,N*-dimethylaniline has been investigated making use of electrochemistry and NMR spectroscopy. The ambient temperature chloroaluminate molten salt, composed of 1-ethyl-3-methylimidazolium chloride, ImCl, and aluminum chloride, is the underlying Lewis acid substrate, to which a proton source, $ImHCl_2$, is added. DMA is oxidized in both the basic and acidic melts in the absence of proton and forms an $AlCl_3$ adduct in an acidic (excess $AlCl_3$) melt; the potential for oxidation in the acidic melt is considerably more positive than that in the basic melt. Upon addition of proton, the DMA oxidation wave disappears. In a basic melt (excess ImCl), an amperometric titration indicates that DMA reacts quantitatively with protons, added as $ImHCl_2$, to form $DMAH^+$, which is not oxidized in the melt window. ^{13}C and ^1H NMR spectroscopy show changes in chemical shifts consistent with these observations. $DMAH^+$ shows a reduction wave at potentials more negative than that shown by "free" proton reduction in the basic melt; reverse pulse voltammetry from the limiting plateau for this reduction wave shows a H_2 oxidation wave and reappearance of the DMA oxidation wave. These results indicate that the process corresponds to the reduction of the proton from the $DMAH^+$, to yield H_2 and DMA at the electrode surface. In an acidic melt, DMA forms an $AlCl_3$ adduct; on addition of proton, a $DMAH^+$ species, which cannot be oxidized in the melt window, is formed. However, the reaction of the DMA-$AlCl_3$ adduct in the acidic melt with proton appears to be less quantitative than the reaction of proton with DMA in the basic melt. Again, the ^{13}C and ^1H NMR support these observations.

In this paper, we report on chemistry in a unique "superacid" solvent, in which the variation of the underlying Lewis acidity of the solvent is employed to vary the Brønsted acidity of protons in the solvent. *N,N*-Dimethylaniline is used as a probe molecule to investigate this unusual solvent system.

In our own studies of ambient temperature molten salts, consisting of aluminum chloride together with an organic chloride, either *N*-butylpyridinium chloride (BuPyCl) or 1-ethyl-3-methylimidazolium chloride (ImCl), we noted that very large shifts in the potential for proton reduction, of the order of 1.5 V, were observed as the melt composition was varied from acidic (excess $AlCl_3$) to basic (excess organic chloride);[1] these shifts in potential could be correlated by donor-acceptor theory to imply a large change in the donicity of the underlying solvent.[2,3] Recent work by Smith and co-workers determined Hammett acidity functions, H_0, for protons in acidic ImCl-$AlCl_3$ melts and found that in a "slightly" acidic melt, proton, added as HCl(g) at 0.01 atm, exhibits an H_0 value of -12.6, while in a melt saturated with $AlCl_3$ (~67 mol % $AlCl_3$), the H_0 value is -18 for 1 atm of HCl(g).[4,5] The protons in these melts are more acidic than 100% H_2SO_4 (H_0 = -12), which is arbitrarily assigned as the lower limit for superacidity.[6] Thus, protons in the ambient temperature acidic melts may be considered Brønsted superacids.

The use of "superacid" solvents as media for electrochemical studies is not widespread; studies appear to be limited to the electrochemical oxidation of alkanes.[7,8] A review has also appeared in which the standard potentials of alkane redox couples are calculated from free energies of formation.[9]

Earlier work in our laboratory on the electrochemistry of anthracene[10] and a variety of amines[11] in these molten salts had indicated the possible formation of $AlCl_3$ adducts, particularly in acidic melts. We concluded, at that time, that dimethylaniline formed an aluminum chloride adduct in the acidic melt and that anthracene, based on spectral observations, did likewise. However, it was suggested to us, and subsequently confirmed, that, in the case of anthracene, we were likely observing the formation of protonated anthracene as a result of the presence of protonic impurities.[12] In fact, anthracene was used by Smith as one of the bases employed in his study of Hammett acidity in these chloroaluminate melts.[5] However, our results on the behavior of the organic amines, and later quinones,[13,14] appeared to indicate the formation of $AlCl_3$ adducts.

Our initial goal in the present work was to see if the deliberate and quantitative addition of proton, from $ImHCl_2$, to these melts would affect the electrochemistry of organic bases, in this case dimethylaniline. In acidic melts, where we had proposed the existence of a DMA-$AlCl_3$ adduct, we wished to see if the proton would replace the $AlCl_3$ on the base. To investigate this further, we carried out ^1H and ^{13}C NMR spectroscopy on the DMA in the molten salts in the presence and absence of added proton and under a variety of conditions. The results of these experiments are presented here.

Experimental Section

All experiments were carried out in a Vacuum Atmosphere drybox under a Helium atmosphere. 1-Ethyl-3-methylimidiazolium chloride was synthesized following reported procedures;[15] aluminum chloride (Fluka,

† Present Address: Department of Industrial Chemistry, Chungbuk National University, Cheongju-city, Chungbuk, 360-763 Korea.
‡ Present Address: Department of Chemistry, University of Alabama, Tuscaloosa, Alabama 35487.

(1) Sahami, S.; Osteryoung, R. A. *Anal. Chem.* **1983**, *55*, 1970.
(2) Gutmann, V. *The Donor-Acceptor Approach to Molecular Interactions*; Plenum Press: New York, 1978.
(3) Zawodzinski, T. A., Jr.; Osteryoung, R. A. *Inorg. Chem.* **1989**, *28*, 1710.
(4) Smith, G. P.; Dworkin, A. S.; Pagni, R. M.; Zingg, S. P. *J. Am. Chem. Soc.* **1989**, *111*, 5075.
(5) Smith, G. P.; Dworkin, A. S.; Pagni, R. M.; Zingg, S. P. *J. Am. Chem. Soc.* **1989**, *111*, 525.
(6) Olah, G. A.; Prakash, G. K. S.; Sommer, J. *Superacids*; Wiley: New York, 1985.
(7) Bertram, J.; Coleman, J. P.; Fleischmann, M.; Pletcher, D. *J. Chem. Soc., Perkin Trans. II* **1973**, 374.
(8) Devynck, J.; Farbre, P. L.; Hadid, A. B.; Tremillon, B. *J. Chem. Res. Synop.* **1979**, 200.
(9) Farbre, P. L.; Devynck, J.; Tremillon, B. *Chem. Rev.* **1982**, *82*, 591.
(10) Robinson, J.; Osteryoung, R. A. *J. Am. Chem. Soc.* **1979**, *101*, 323.
(11) Robinson, J.; Osteryoung, R. A. *J. Am. Chem. Soc.* **1980**, *102*, 4415.
(12) Zingg, S. P.; Dworkin, A. S.; Sorlie, M.; Chapman, D. M.; Buchanan, A. C., III; Smith, G. P. *J. Electrochem. Soc.* **1984**, *131*, 1602.
(13) Cheek, G. T.; Osteryoung, R. A. *J. Electrochem. Soc.* **1982**, *129*, 2488.
(14) Uribe, F. A.; Osteryoung, R. A. *J. Electrochem. Soc.* **1988**, *135*, 378.
(15) Wilkes, J. S.; Levisky, J. A.; Wilson, R. A.; Hussey, C. L. *Inorg. Chem.* **1982**, *21*, 1263.

0002-7863/91/1513-3334$02.50/0

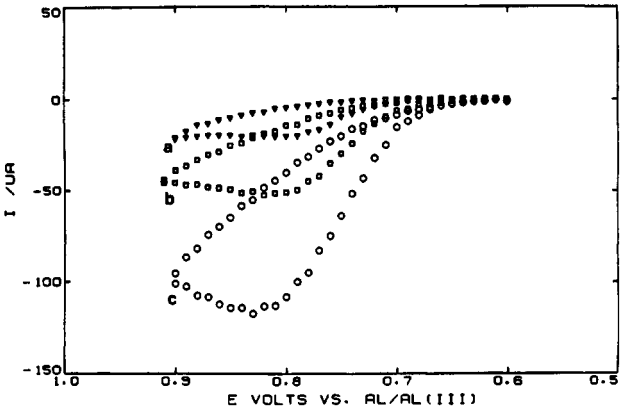

Figure 1. Staircase cyclic voltammogram for DMA in the 0.8:1 melt at a Pt electrode, $A = 2 \times 10^{-2}$ cm^2: scan rate 250 mV s^{-1} (step height 10 mV, step width 40 ms); [DMA] = 10.4 (a), 29.7 (b), 52.8 mM (c).

iron free) was purified by sublimation. The molten salt 1-ethyl-3-methylimidazolium hydrogen dichloride ($ImHCl_2$) was prepared from direct reaction of ImCl and HCl(g).[16] Methyl aluminum sesquichloride (MAC, $Me_3Al_2Cl_3$) was obtained from Aldrich and used without further purification.

Cyclic voltammetric studies were performed with an EG&G PARC Model 175 universal programmer with a Model 173 potentiostat/galvanostat. Voltammograms were plotted on a Houston Instruments Model 200 X-Y recorder. All other electrochemical studies were carried out with an EG&G Model 273 potentiostat/galvanostat controlled by a DEC PDP-8/e computer.[17] An LNO3 Plus laser printer was used to obtain plots from the computer experiments.

For cyclic and pulse voltammetric studies, Pt disk (radius 0.08 cm) or glassy carbon (GC) electrodes (radius 0.15 cm) were used. The electrodes were obtained from Bioanalytical Systems. For all melt electrochemical measurements the reference electrode was an Al wire (5N Alfa Inorganics) immersed in a 1.5:1 $AlCl_3$–ImCl melt in a separate fritted glass compartment. The counter electrode was a coiled Al wire.

Rotating ring–disc voltammetric experiments were carried out with a four-electrode system with a Pine Instruments Pt–Pt ring–disk electrode ($r_1 = 0.09$ cm; $r_2 = 0.097$ cm; $r_3 = 0.101$ cm). A Pine Instrument RDE-4 potentiostat was used.

^{1}H NMR experiments were performed with either a Varian Gemini-300 or a Varian VXR-400 S spectrometer operating at 300.075 or 399.952 MHz, respectively. ^{13}C NMR experiments were performed with broad-band proton decoupling on the instruments indicated above operating at 75.462 and 100.57 MHz, respectively. ^{1}H and ^{13}C samples of the melts were prepared in the drybox and pipetted into 5-mm tubes fitted with precision coaxial inserts (Wilmad Glass Co.). They were then capped and sealed with Parafilm prior to removal from the drybox. ^{1}H and ^{13}C chemical shifts are reported relative to 0.1% TMS in $CDCl_3$ in the coaxial insert.

Results and Discussion

I. Electrochemistry and NMR Spectroscopy of *N,N'*-Dimethylaniline (DMA) and Protonated DMA ($DMAH^+$) in 0.8:1.0 $AlCl_3$–ImCl. Staircase cyclic voltammetry was performed to obtain an overview of the DMA electrochemical behavior in the presence and absence of deliberately added protons. In this basic melt, the anodic limit results from the oxidation of chloride ion.[18] Figure 1 shows a staircase cyclic voltammogram of DMA at a Pt electrode in the basic melt; the open circuit potential of the Pt electrode with DMA in solution is ca. +0.2 V. An oxidation wave at 0.75 V is observed which is near the melt's anodic limit. No reduction waves associated with the DMA oxidation are observed upon scan reversal. In our previous investigation of DMA in a "slightly basic" BuPyCl–$AlCl_3$ melt, the oxidation wave of DMA was associated with two reduction waves.[11] These resulted from the coupling of two oxidized DMA units to form tetramethylbenzidine, TMB, which was immediately oxidized to the dication, TMB^{2+}. The two reduction waves resulted from the reduction of the TMB^{2+} to TMB in two one-electron steps. With increasing chloride concentration, TMB^{2+} was found to become unstable and no cathodic peaks were observed. In the 0.8:1.0 basic melt employed in this work, the chloride concentration is sufficiently large, ca. 1 M, so that no cathodic waves corresponding to TMB^{2+} are found. On the basis of the previous work, however, we assume that the DMA oxidation is still a 2-electron process.[11]

Table I. $E_{1/2}$ and Limiting Current Variation with Pulse Width for 52.8 mM DMA in 0.8:1.0 $AlCl_3$–ImCl Melt at Pt and GC Electrodes

	Pt		GC	
t_p, ms	$-i_{lim}$,[a] μA	$E_{1/2}$, V	$-i_{lim}$,[b] μA	$E_{1/2}$, V
1000	45.1	0.74	140	0.76
750	51.3	0.77	162	0.76
500	65.7	0.78	209	0.77
250	91.5	0.79	297	0.79
100	140	0.81	472	0.81
75	164	0.83	527	0.82
50	233	0.84		

[a] $it_p^{1/2} = (46.1 \pm 2.7) \times 10^{-6}$ A s$^{1/2}$. [b] $it_p^{1/2} = (145 \pm 4)^{1/2} \times 10^{-6}$ A s$^{1/2}$.

Normal pulse (NP) voltammograms were obtained as a function of pulse width and DMA concentration. In these NP experiments, the initial surface boundary conditions were reestablished after each pulse by holding the electrode at the open-circuit potential and stirring the solution for 2 s, followed by a waiting period of 8 s, prior to each new pulse application. Well-defined normal pulse waves were obtained, and the relevant parameters obtained from these experiments for a solution 53 mM in DMA are summarized in Table I for Pt and GC electrodes. As t_p decreases, $E_{1/2}$ is observed to shift anodically.

Plots of i_{lim} for the normal pulse experiments vs [DMA], for 50 and 100 ms pulse widths, are linear but have an identical nonzero intercept. The nonzero intercept results from the presence of an initial protonic impurity, most likely arising from water, which protonates DMA,[12] forming $DMAH^+$[1] which cannot be oxidized in the melt window. The level of protonic impurities in the basic melt can be estimated directly from the x intercepts of such plots and is of the order of 4 mM.

A diffusion coefficient for DMA can be calculated from the limiting current (Cottrell equation) for the NP voltammograms

$$i_{lim} = nFAC(D/\pi t_p)^{1/2} \quad (1)$$

where n is the number of electrons involved in the process, F is the Faraday constant, A is the area of the electrode, C is the concentration of the diffusing species, and t_p is the pulse width.[19] A plot of log i_{lim} vs log t_p is linear with slopes of 0.49 and 0.52 for the Pt and GC electrodes, respectively, indicating the limiting current is diffusion controlled. Because the concentration of DMA undergoing oxidation in these experiments is somewhat less than that added, as discussed above, plots of i_{lim} vs C, which have slopes independent of C, should provide more accurate values for the DMA diffusion coefficients than plots of i_{lim} vs $t_p^{-1/2}$. Diffusion coefficients from the plot of the [DMA] vs i_{lim} at Pt were found to be 1.92×10^{-7} and 1.60×10^{-7} cm^2 s^{-1} for pulse widths of 100 and 50 ms, respectively, assuming an n value of 2. If the protonic impurity concentration were taken as 4 mM, as indicated above, then, using a corrected value of [DMA] of 49 mM, a value of D was calculated from a plot of i_{lim} vs $t_p^{-1/2}$. These values were 1.59 and 1.57×10^{-7} cm^2 s^{-1}, for the Pt and GC electrodes, respectively. ($i_{lim} = (148.3 \times 10^{-6})t_p^{-1/2} - 1.87 \times 10^{-6}$ and $(42.8 \times 10^{-6})t_p^{-1/2} + 2.85 \times 10^{-6}$ for GC and Pt, respectively.)

A ^{13}C NMR spectrum for the methyl carbons is shown in Figure 2 for neat DMA (spectra a) and DMA in the basic melt (spectra b); the chemical shifts are identical and show that DMA does not form an $AlCl_3$ adduct in the basic melt.

Upon addition of proton, significant changes in the electrochemistry of DMA take place. Staircase cyclic voltammograms

(16) Zawodzinski, T. A.; Osteryoung, R. A. *Inorg. Chem.* **1989**, *27*, 4383.
(17) Brumleve, T. R.; O'Dea, J. J.; Osteryoung, R. A.; Osteryoung, J. *Anal. Chem.* **1981**, *53*, 702.
(18) Lipsztajn, M.; Osteryoung, R. A. *J. Electrochem. Soc.* **1983**, *130*, 1968.
(19) Parry, E. P.; Osteryoung, R. A. *Anal. Chem.* **1965**, *37*, 1654.

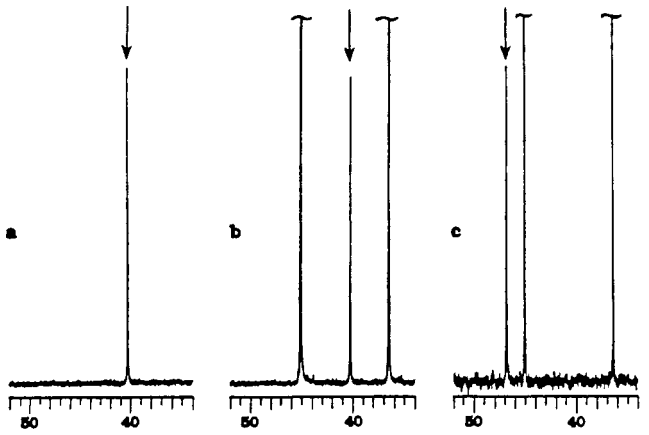

Figure 2. ^{13}C spectrum of methyl carbons from DMA in (a) neat DMA, (b) basic melt, and (c) acidic melt. Off-scale peaks without arrows in b and c are from the imidazolium cation.

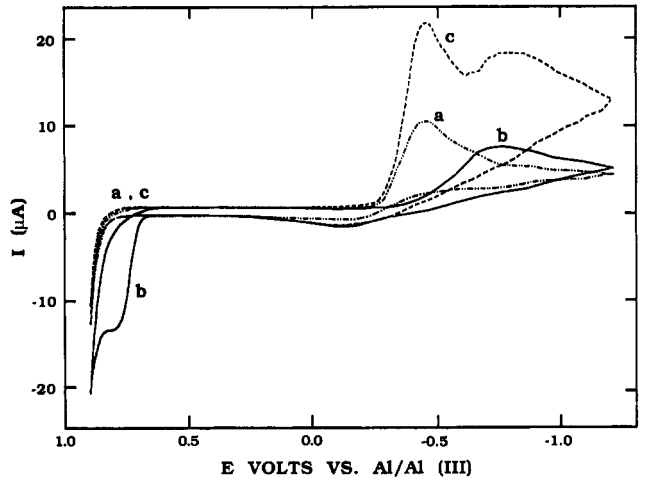

Figure 3. Staircase cyclic voltammograms for DMA in the 0.8:1 melt: (a) melt background; (b) 17 mM DMA added; (c) as in b, but 30 mM $ImHCl_2$ added. Conditions as in Figure 1. Sweep rate 100 mV s^{-1} (step height 10 mV, step width 100 ms).

at a Pt electrode for a melt containing no DMA, added DMA, and then proton, added as $ImHCl_2$, a quantitative source of proton,[16] are shown in Figure 3. Figure 3a shows the melt with no added DMA; a cathodic wave at ca. −0.4 V is seen and is due to the presence of protonic impurities.[1] Upon addition of DMA, Figure 3b, the wave at −0.4 V disappears, a new cathodic wave, at −0.7 V, appears, and the anodic DMA oxidation wave can be seen. The wave at −0.7 V appears to be due to the reduction of proton from the protonated DMA (see below). On addition of $ImHCl_2$ in excess of the amount of DMA present, Figure 3c, the DMA oxidation wave disappears, and, on a cathodic going scan, reduction waves for "free" proton and an increase in the protonated DMA wave are seen. In a basic melt, "free" protons exist largely as HCl_2^-.[16]

Although DMA oxidation is found at a GC electrode, no cathodic waves are seen. Protons cannot be reduced in the melt at the GC surface,[1] and apparently the $DMAH^+$ is also not reducible on this surface.

To quantitate the reaction between DMA and proton, an amperometric titration, monitoring the change of the DMA oxidation wave as $ImHCl_2$ was added, was carried out. $ImHCl_2$ was added to the solution initially 53 mM in DMA (though the solution, as per the data presented above, contains only 49 mM of "free" DMA). The DMA oxidation limiting current decreases linearly with added $ImHCl_2^-$, indicating a quantitative reaction with the DMA. The current goes to zero after the solution is ca. 55 mM in $ImHCl_2$. ($i_{lim} = 172.0 \times 10^{-6} - 3.126 \times 10^{-3}[ImHCl_2]$; i = 0 at $[ImHCl_2]$ = 55 mM.) On the basis of the argument presented above, only 49 mmol of "free" DMA was in solution; thus the intercept in the titration presents an error of ca. 12% assuming 1:1 stoichiometry in the reaction of DMA with proton. This, however, seems quite reasonable, in part the result of weighing errors in adding the $ImHCl_2$ to the melt and in part, perhaps, due to the lack of complete stoichiometry in the $ImHCl_2$.

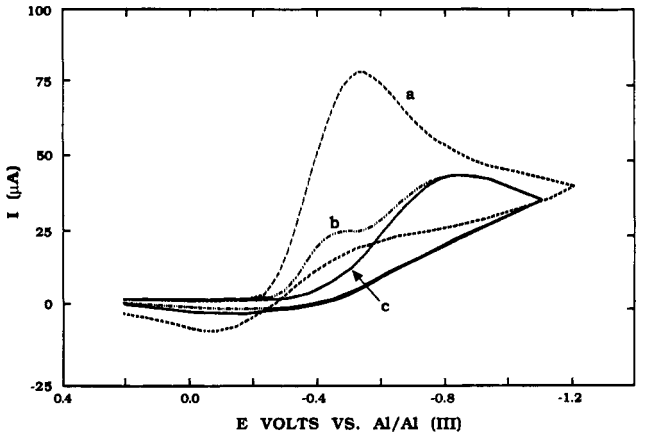

Figure 4. Cathodic staircase cyclic voltammetry for the 0.8:1 melt as MAC is added to the melt initially 53 mM in DMA and 107 mM in $ImHCl_2$: [MAC] = 13.7 (a), 49.8 (b), 75 mM (c). Other conditions as in Figure 1.

Adding methylaluminum sesquichloride, MAC, to the DMA solution containing excess proton also resulted in marked changes in staircase cyclic voltammetry of the DMA. MAC, like ethylaluminum chloride, is an effective reagent for proton removal.[20] The staircase voltammograms, Figure 4, initially showed only one reduction wave at a potential characteristic of the free proton (part a); although reduction of both free protons and the proton from $DMAH^+$ should have been seen in Figure 4a, it is obvious that only one wave is seen. It may have been swamped by the very large first wave; these proton waves are not all that well behaved. As more MAC was added, two reduction waves, corresponding to the free proton reduction and the proton on the $DMAH^+$, appeared (Figure 4b). As still more MAC was added, the free proton reduction wave disappeared, leaving only the $DMAH^+$ reduction wave (Figure 4c). The $DMAH^+$ wave decreased slowly with time, indicating a sluggish reaction of the $DMAH^+$ with MAC. The DMA oxidation wave was also observed to reappear with addition of MAC, albeit with lower current than expected. However, DMA appears to slowly decompose in the melt over long times which may explain this observation.

To further examine the $DMAH^+$ reduction, reverse pulse voltammetry was carried out at a Pt electrode.[21] In this experiment, the electrode potential is stepped from an initial value, E_i, of +0.2 V to −1.1 V for a generation time, τ, after which it is stepped to increasingly positive potentials in 2.0-mV increments for a time t_p, the analysis pulse, to examine the oxidation of products generated during the $DMAH^+$ reduction. After each generation and analysis pulse, the solution was stirred for 2.1 s and then maintained in a quiet state for 5.9 s to renew the surface concentrations. A NP oxidation wave for DMA containing solution and a RP wave for the same solution are shown in Figure 5, a and b. As should be the case if t_p values for the NP and RP experiments are the same, the two oxidation waves coincide. Also shown is the RP voltammogram resulting when the concentration of $ImHCl_2$ added was approximately equal to that of the DMA (Figure 5c). At the −1.1 V generating potential, the $DMAH^+$ is reduced, as discussed above. A slight "dc" cathodic current is seen on the reverse pulse voltammogram. We assign the first oxidation wave, starting at −0.2 V, to the oxidation of H_2 generated during the reduction, while the second oxidation wave is at the same potential as that for the DMA oxidation. Since no excess

(20) Zawodzinski, T. A.; Carlin, R. T.; Osteryoung, R. A. *Anal. Chem.* **1987**, *59*, 2639.
(21) Osteryoung, J.; Kirowa-Eisner, E. *Anal. Chem.* **1980**, *52*, 62.

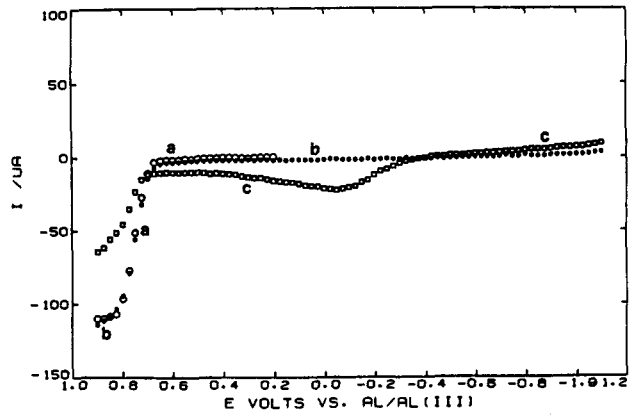

Figure 5. NP and RP waves for the 0.8:1 melt containing DMA and DMA + $ImHCl_2$. Pulse width 50 ms; delay time between pulses 8 s (2.1 s stirred, 5.9 s quiescent): (a) NP – 36.2 mM DMA; (b) RP on the same solution from −1.1 V, generation time at −1.1 V, 5 s; (c) RP from −1.1 V on the same solution but after 36.8 mM $ImHCl_2$ is added; generation time at −1.1 V 5 s.

HCl_2^- is present, the H_2 arises from the $DMAH^+$ proton reduction; the DMA is liberated from the proton adduct at the same time, and its oxidation is seen as well. The H_2 oxidation is at a more positive potential than previously indicated by cyclic voltammetry;[1] this is probably due both to the fact that the reference electrode employed here is ca. 180 mV more negative than that previously employed and also the fact that the short pulse voltammetric t_p value shifts the rather irreversible process to more positive potentials. The reaction taking place during the $DMAH^+$ reduction, therefore, may be written as

$$DMAH^+ + e = DMA + \tfrac{1}{2}H_2 \qquad (2)$$

It was not possible to quantitate the reverse pulse voltammetry due to the absence of theory and also, as indicated above, the lack of quantitatively reproducible voltammograms. Qualitatively, however, similar behavior was always observed.

Some rotating ring–disc voltammetry was carried out to confirm the above observations with an additional experimental procedure. Rotating disc voltammograms in the basic melts were not well-defined; at higher rotation rates (>400 rpm) ill-defined limiting currents for DMA oxidation were obtained. In the neutral melt, however, due to the shift in the background current for Cl^- oxidation, very well defined limiting currents were obtained. A plot of the limiting current against the square root of the rotation rate was linear and passed through the origin, indicating adherence to the Levich equation. A cyclic staircase voltammogram run in the neutral melt indicated the presence of the coupling product of DMA, as seen in our previous work in this area,[11] rather than the 2-electron, irreversible oxidation seen in the basic melts employed above.

A series of ring voltammograms at a Pt–Pt electrode are shown in Figure 6 for an experiment in a basic 0.8:1.0 melt. Comparison is made between a ring scan with the disc open-circuited and with the disc held at increasingly cathodic potentials to reduce the protonated $DMAH^+$. The melt contains an excess of DMA over proton, added as $ImHCl_2$. Two features are noted. First, as the potential of the disc is made increasingly negative, an increase in the DMA oxidation current is clearly noted. The current also ceases to increase for disc potentials more negative than −0.9 V. Second, a slight anodic current is noted in the vicinity of zero volts, which we attribute to the oxidation of H_2 formed during the $DMAH^+$ reduction at the disc.

Although ring–disc experiments in a melt containing close to the same amounts of DMA and $ImHCl_2$ were carried out, similar to those in the reverse pulse voltammetric experiments of Figure 5, the results showed only a slight shift in the current at the anodic limit, rather than a clear-cut difference as shown in the experiments with the excess DMA present. Nevertheless, the rotating-ring–disc experiments are, qualitatively, in accord with the reverse pulse experiments which, however, show much better

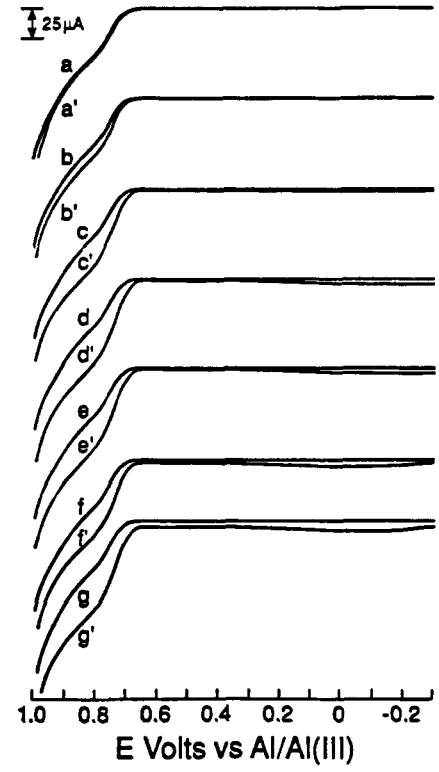

Figure 6. Ring voltammograms for DMA in basic melt: [DMA] = 54 mM; [$ImHCl_2$] = 31 mM; ring scan rate 10 mV s^{-1}; (a–g) Ring voltammogram with disc at open circuit; (a′–g′) ring voltammogram with disc at (a′) −0.5 V, (b′) −0.7 V, (c′) −0.9 V, (d′), −1.1 V, (e′) −1.3 V, (f′) −1.5 V, (g′) −1.7 V.

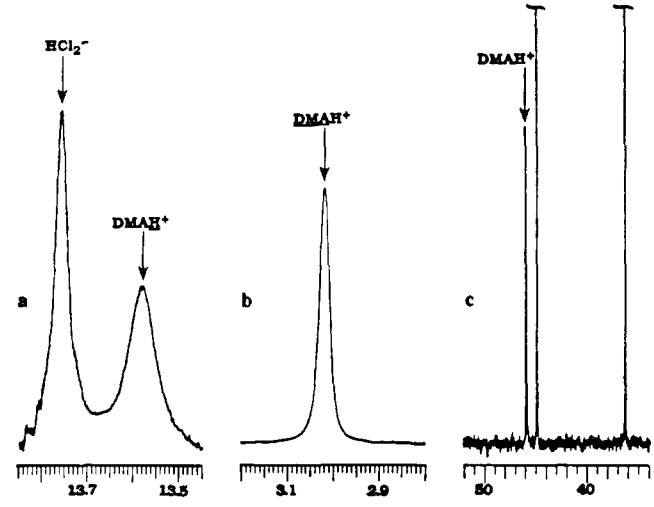

Figure 7. ^{13}C and ^1H spectra of DMA in basic melt following addition of $ImHCl_2$ in excess of DMA: (a) ^1H spectrum for proton on DMA, i.e., $DMAH^+$ and HCl_2^-; (b) ^1H spectrum for methyl protons; (c) ^{13}C spectrum of methyl carbons. The offscale peaks without arrows in c are from the imidazolium cation.

defined oxidation waves than are seen at the ring.

The ^{13}C spectrum for the methyl carbons on addition of proton to DMA in a basic melt is shown in Figure 7c. Under conditions where an excess of proton is in solution, i.e., only $DMAH^+$ is in solution, the resonance is at 46 ppm (vs TMS), compared to 41 ppm for DMA in the basic melt. The ^1H spectrum, Figure 7a, shows a line for HCl_2^-, at 13.76 ppm, and a line at 13.57 ppm which we attribute to proton on the amine nitrogen; this indicates exchange between the two species is slow on the NMR time scale. However, only a single line, at 3.01 ppm, is observed in Figure 10b for the methyl protons, although a doublet is expected, and is seen in the acidic melt (see below); this single line indicates some

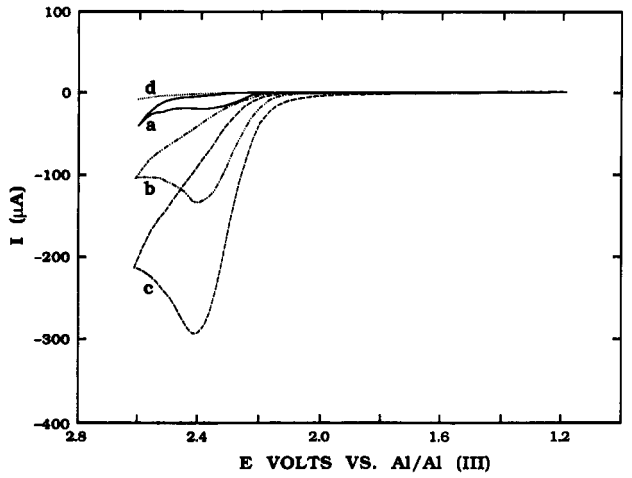

Figure 8. Staircase cyclic voltammetry for DMA in acidic (1.2:1) melt: GC electrode, $A = 7.07 \times 10^{-2}$ cm^2; scan rate 250 mV s^{-1} (step height 10 mV, step width 40 ms); [DMA] = 8.1 (a), 18.5 (b), 30.3 mM (c), melt background (d).

exchange and an approach to the slow exchange limit.

Basic melts containing known, but varying, amounts of both DMA and protonated DMAH$^+$ can be formed, as shown previously, by adding $ImHCl_2$ to a melt initially containing only DMA. In such melts, a single ^{13}C line is found, the position of which is proportional to the population weighted average of the species present. This indicates that the exchange between the protonated and unprotonated DMA is fast on the NMR time scale.

Proton transfers involving nitrogen bases are almost always very fast.[22] The fast proton exchange observed in basic melts containing DMA and DMAH$^+$ is, therefore, as expected. Under certain circumstances, namely in highly acidic media, proton transfer to nitrogen can be made to appear slow. In the case of DMA, apparent slow proton transfer has been observed in concentrated perchloric acid.[23] The proton transfer, in fact, remains fast but the highly acidic medium inhibits the separation of the proton-transfer products. It appears that this is what is occurring when proton exchange approaching the slow exchange limit is observed in basic melts containing HCl_2^- and DMAH$^+$.

The quantitative reaction of proton in the form of HCl_2^- with DMA in the basic melt is not surprising. DMA is expected to be a stronger base toward proton than is the chloride ion. We have previously estimated the donor number of a basic melt as 26.[3] While we have been unable to find a donor number for DMA, one may be inferred from data in the literature, a donor number estimate of ca. 34.[24] While certainly not compelling, the trend is at least in the right direction. Apparently the stability of the $AlCl_4^-$ prevents the DMA from disrupting its coordination sphere; this may be due to the larger steric requirements of the DMA vs Cl^-, or simply that the donor number differences are too small for the displacement to occur.

II. Electrochemistry and NMR Spectroscopy of DMA and Protonated DMA in Acidic $AlCl_3$–ImCl. Staircase cyclic voltammograms for the oxidation of DMA at GC are shown in Figure 8. The peak currents occur at 2.5 V, near the acidic melt anodic limit at the GC electrode. The potential for the oxidation of Cl^- from $AlCl_4^-$, the limiting reaction in an acidic melt, is ca. 0.5 V more positive on GC than on Pt, thus forcing these studies to be carried out at GC electrodes.

The oxidation potential of DMA in the 1.2:1.0 $AlCl_3$–ImCl melt is ca. 1.75 V more positive than in the basic melt. This effect was attributed in our previous study to the formation of a DMA–$AlCl_3$ adduct in the acidic melt. Thus, in the acidic melt, the reaction

$$Al_2Cl_7^- + DMA = DMA\text{–}AlCl_3 + AlCl_4^- \qquad (3)$$

takes place. As indicated previously, no such complexation is observed in the basic melt. The Lewis acid, $AlCl_3$, removes electron density from the DMA molecule, making it more difficult to oxidize.

The ^{13}C spectrum of the methyl carbons in the acidic melt is shown in Figure 2c. A shift to 47 ppm is seen, compared to 41 ppm in the basic melt. We take this to show the presence of an $AlCl_3$ adduct.

From eq 3, if more DMA than $Al_2Cl_7^-$ is added to a slightly acidic melt, the resulting melt will contain both the DMA–$AlCl_3$ adduct and free DMA. The melt itself, formally, may be considered neutral in terms of its Lewis acidity. A single ^{13}C peak for the DMA methyl carbons is found; the position of this peak is proportional to the population weighted average of the two DMA species present. This indicates that the exchange between the free DMA and the $AlCl_3$ adduct is fast on the NMR time scale.

The DMA limiting current was monitored as a function of DMA concentration, and, as in the basic melts, plots of i_{lim} from normal pulse voltammetry vs [DMA] had nonzero intercepts. From the x intercept, the concentration of an impurity (proton) was estimated to be 7.4 mM. The higher impurity level in the acidic melt may result from a difference in the quality of the reagents or from the greater scavenging ability of the acid melt for adventitious water in the drybox. From the slope of i_{lim} vs [DMA] the diffusion coefficient of DMA in the acidic melt is calculated to be 8.4 and 9.1 $\times 10^{-7}$ cm^2 s^{-1} for 50 and 100 ms pulse widths, respectively. From the slope of i_{lim} vs $t_p^{-1/2}$ plots, the diffusion coefficient is calculated to be 5.5 and 6.9 $\times 10^{-7}$ cm^2 s^{-1}, for 30.3 and 50.5 mM DMA, respectively. If these latter values were corrected for the 7.4 mM DMA initially tied up with proton, values of 9.7 and 9.5 $\times 10^{-7}$ cm^2 s^{-1} for the 30 and 50 mM solutions, respectively, were obtained. These values are in good agreement with those from the i_{lim} vs [DMA] plots. The values are about five times greater than those in the basic melt. Solely on the basis of viscosity effects, the diffusion coefficient of the DMA would be two to three times larger in the acidic melt than in the basic melt.[25]

Normal pulse parameters in the 1.2:1 melt for a 30.3 and 50.5 mM DMA are summarized in Table II. Values of $it_p^{1/2}/C_{DMA}$ are tabulated for the [DMA] corrected for the protonic impurity and are quite constant. The value of the ratio of the limiting currents for the two concentrations of DMA is also in good agreement with the ratio of the concentrations of DMA if these concentrations are corrected for the ca. 7 mM protonic impurity which effectively removes the DMA from the melt as discussed above.

Addition of $ImHCl_2$ to the acidic melt containing DMA results in a marked decrease in the DMA oxidation wave at +2.5 V; we assume this is due to the replacement of the $AlCl_3$ by a proton on the DMA. Cyclic staircase voltammograms for this are shown in Figure 9. However, here the DMA oxidation wave does not

Table II. $E_{1/2}$ and Limiting Current Variation with Pulse Width for 30.3 and 50.5 mM DMA in 1.2:1.0 $AlCl_3$–ImCl melt at the GC Electrodes

t_p ms	$-i_{lim}$,[a] μA	$E_{1/2}$, V	$-i_{lim}$,[b] μA	$E_{1/2}$, V	$i_{lim}(50.5)/i_{lim}(30.3)$[c]
1000	162	2.27	309	2.29	1.90
750	187	2.28	361	2.30	1.93
500	224	2.29	449	2.31	2.00
250	346	2.31	664	2.34	1.92
100	520	2.34	993	2.37	1.91
75	621	2.36			
50	751	2.37			
25	993	2.40			

[a] $it_p^{1/2}/C_{Corr} = (7.18 \pm 0.24) \times 10^{-6}$ A s$^{1/2}$. [b] $it_p^{1/2}/C_{corr} = (7.35 \pm 0.20) \times 10^{-6}$ A s$^{1/2}$. [c] Ratio of concentrations added (50.5/30.3) = 1.66; ratio f concentrations corrected for loss of initial DMA due to ca. 7.4 mM proton impurity (see text) ((50.5 - 7.4)/(30.4 - 7.4)) = 1.88.

(22) Kresge, A. J. *Acc. Chem. Res.* **1975**, *8*, 354.
(23) Kresge, A. J. *J. Am. Chem. Soc.* **1975**, *97*, 1795–1797.
(24) Makitra, R. G.; Pirio, Zu. N.; Sendeoa, R. V.; Turkevich, O. E.; Dokl. *Akad. Nauk Atr. RSR: Ser. B: Geal. Khim. Biol. Nauki.* **1976**, *11*, 998.
(25) Fannin, A. A., Jr.; Floreani, D. A.; King, L. A.; Sanders, J. S.; Piersma, B. J.; Stech, D. J.; Vaughn, R. L.; Wilkes, J. S.; Williams, J. L. *J. Phys. Chem.* **1984**, *88*, 2614.

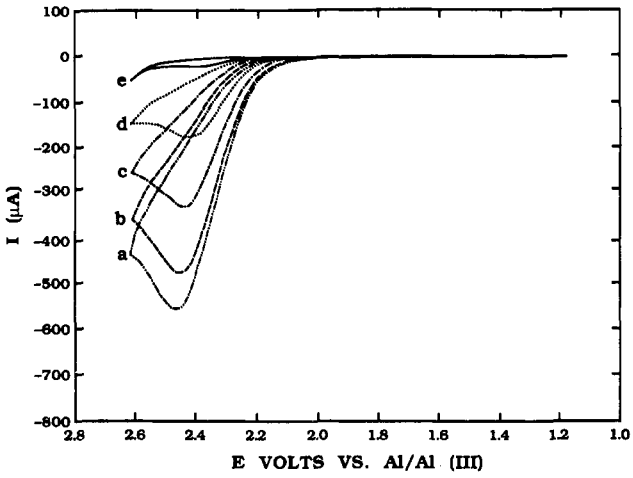

Figure 9. Staircase cyclic voltammogram for DMA in acidic melt, as $ImHCl_2$ is added: conditions as in Figure 8; [DMA] = 50 mM, [$ImHCl_2$] = 0 (a), 10.1 (b), 29.3 (c), 51.5 (d) and 80.5 mM (e).

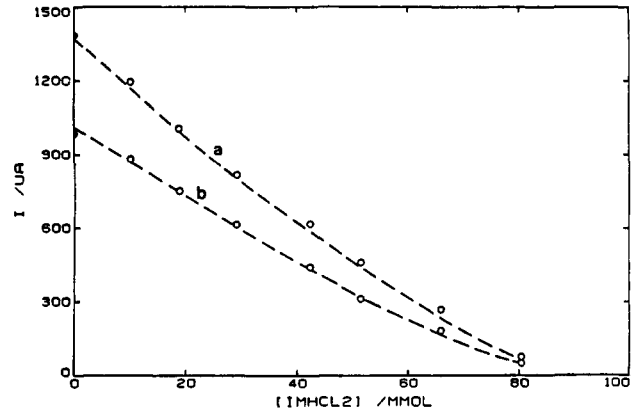

Figure 10. Normal pulse limiting current for DMA oxidation vs [$ImHCl_2$] added to melt: initial [DMA] = 50.5 mM; t_p = 50 (a) and 100 ms (b).

disappear when an amount of $ImHCl_2$ equivalent to the DMA has been added. A plot of the i_{lim} for a normal pulse voltammogram of DMA vs [$ImHCl_2$] added is shown in Figure 10. The initial decrease of the DMA oxidation current is linear, but it then shows marked curvature, and an extrapolation to the [$ImHCl_2$] axis yields an intersection well in excess of the amount (50 mmol) of DMA present in solution. This indicates the presence of an equilibrium between a DMA–$AlCl_3$ adduct and a protonated DMA adduct, $DMAH^+$.

As previously reported, if excess proton were added to an acidic melt containing DMA, i.e., to the DMA–$AlCl_3$ species, the methyl ^{13}C peak shifts downfield by 1.5 ppm, to 48.5 ppm, and a new ^1H line at 7.8 ppm, vs TMS, is seen.[26] A split in the methyl protons, indicative of coupling, is also seen. (Irradiation of the 7.8-ppm line results in a collapse of the doublet, clearly indicating coupling of the two peaks.) These results are shown in Figure 11. The chemical shifts for the ^1H peak for $DMAH^+$ in the basic and acidic melt are at 13.6 and 7.8 ppm vs TMS, respectively. We believe that the large difference results from the interaction of the proton on the DMA with chloride ion in the basic melt, perhaps as a result of hydrogen bond formation. NMR chemical shifts for the imidazolium ring hydrogen as a function of composition in the basic melt have been observed;[27] these, as well as infrared spectral changes in the basic melt, have been ascribed to chloride forming hydrogen bonds with the acidic ring hydrogens.[28-30]

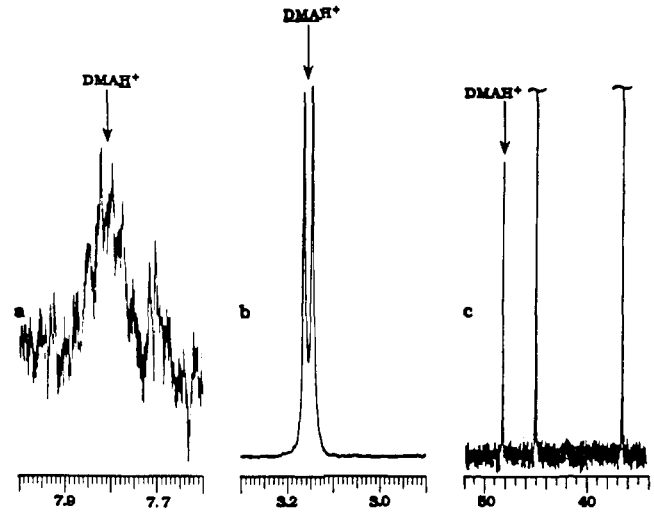

Figure 11. ^1H (a, b) and ^{13}C (c) NMR spectra for DMA in acidic melt containing proton well in excess of DMA present.

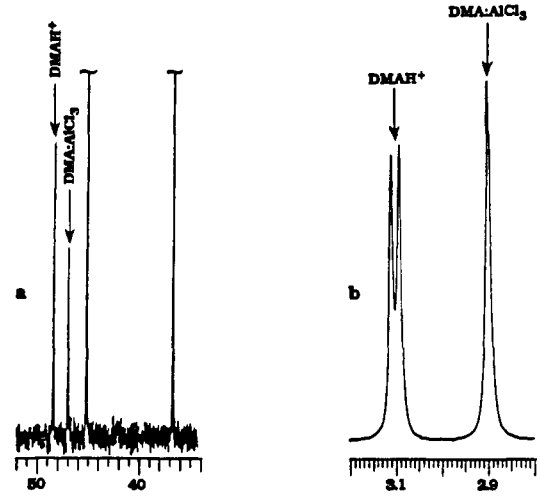

Figure 12. ^{13}C (a) and ^1H (b) NMR spectra for DMA in acidic melt containing DMA in excess of proton.

^1H and ^{13}C NMR spectra for a melt containing both the $DMAH^+$ and the DMA–$AlCl_3$ adduct are shown in Figure 12. Lines for both the protonated and $AlCl_3$ species are clearly evident. This indicates that the exchange between the protonated DMA and the DMA–$AlCl_3$ adduct is slow on the NMR time scale. To our knowledge this is the first NMR observation of a mixture of both a Brønsted and Lewis acid adduct of an organic base.

Of concern is the relative acidity of protons and $Al_2Cl_7^-$ in the melts. To compare relative acidities, it is necessary to remember that the concentration of the $Al_2Cl_7^-$ is ca. 0.86 M in the 1.2:1 melt. Since DMA is complexed by $AlCl_3$ in the acidic melt, the proton versus $Al_2Cl_7^-$ competition reaction may be written as

$$DMA\text{–}AlCl_3 + H^+\cdot\cdot AlCl_4^- = DMAH^+ + Al_2Cl_7^- \quad (4)$$

where $H^+\cdot\cdot AlCl_4^-$ is intended to represent the acidic proton species, whatever it may actually be. Since only small additions of $ImHCl_2$ are required to produce significant decreases in the DMA concentration, the proton competes very effectively for DMA despite the high concentration of $Al_2Cl_7^-$. While the DMA–proton reaction does not appear to be quantitative in the acidic melt, it appears that the equilibrium constant for eq 4 is large.

(26) Trulove, P. C.; Carlin, R. T.; Osteryoung, R. A. *J. Am. Chem. Soc.* **1990**, *112*, 4567.
(27) Wilkes, J. S.; Levisky, J. A.; Pflug, L. J.; Hussey, C. L.; Scheffler, T. B. *Anal. Chem.* **1982**, *54*, 2379.
(28) Tait, S.; Osteryoung, R. A. *Inorg. Chem.* **1984**, *23*, 4352.
(29) Dieter, K. M.; Dymek, C. J., Jr.; Heimer, N. E.; Rovang, J. W.; Wilkes, J. S. *J. Am. Chem. Soc.* **1988**, *110*, 2722.
(30) Dymek, C. J., Jr.; Stewart, J. J. P. *Inorg. Chem.* **1989**, *28*, 1472.

Summary

The results presented indicated that DMA is not complexed in the basic melt but forms an $AlCl_3$ adduct in the acidic melt. The formation of protonated DMA takes place in both basic and acidic melts; the reaction of DMA with proton in the basic melt appears quantitative, while in the acidic melt, where a DMA-$AlCl_3$ adduct is formed, an equilibrium between the protonated species and $AlCl_3$ adduct exists. Both electrochemistry and NMR support these observations.

Acknowledgment. This work was supported by the Air Force Office of Scientific Research. We would also like to acknowledge helpful discussions with Prof. C. D. Ritchie.

Electrochemistry at the Air/Water Interface. Lateral Diffusion of an Octadecylferrocene Amphiphile in Langmuir Monolayers

Deborah H. Charych, Ehud M. Landau, and Marcin Majda*

Contribution from the Department of Chemistry, University of California, Berkeley, Berkeley, California 94720. *Received October 10, 1990*

Abstract: A new electrochemical method is described to investigate the dynamics of lateral diffusion processes in Langmuir monolayers at the air/water interface. The key element of this technique is a gold microband electrode, which can be positioned in the plane of the water surface and which functions as a 1D electrode in contact with a 2D collection of electroactive, water insoluble molecules. Investigations of *N*-octadecylferrocenecarboxamide ($C_{18}Fc$) monolayers and mixed monolayers of $C_{18}Fc$ and octadecanol on 0.05 M $HClO_4$ at 28 °C showed that they remain fluid without undergoing any phase transitions, in a surface concentration range of 3.3×10^{-10} to 7×10^{-11} mol/cm^2. Lateral diffusion of $C_{18}Fc$ can be modeled as a 2D fluid of hard disks with the cross sectional area equal to the projected area of the ferrocene head group. The diffusion coefficient increases linearly with the average free area per molecule on the water surface.

Introduction

This report is concerned with the dynamics of molecular diffusion in 2D systems of Langmuir monolayers at the air/water interface. Our experimental approach is based on electrochemical techniques and relies on a purposefully designed microelectrode, which is positioned in the plane of the air/water interface and which acts as a 1D electrode in this 2D electrochemical experiment. The measurements reported below contribute to the understanding of lateral transport processes and fluidity of biological membranes.[1] In addition, our electrochemical method is capable of providing insight into the kinetics of lateral electron hopping in monolayer assemblies at the air/water interface.

Electrochemical methods are very well suited for the investigation of the dynamics of transport processes, since Faradaic current, even at modest overpotentials, is directly proportional to the arrival rate of the electrochemically active molecules at the electrode surface.[2] We have recently shown the application of electrochemical methods in studies of the lateral diffusion of amphiphiles in organized bilayers produced by self-assembly techniques at Al_2O_3 or glass surfaces.[3,4] The key element in those studies was the development of experimental techniques that allow one to position a working electrode perpendicular to a bilayer assembly. Under such conditions, current can be interpreted in terms of the dynamics of the lateral processes in the bilayer. In this report, we use a similar electrochemical approach to investigate lateral diffusion of a water insoluble *N*-octadecylferrocenecarboxamide ($C_{18}Fc$) at the air/water interface under controlled surface pressure conditions. As in the previous cases, the particular design of a microelectrode that can be positioned at the air/water interface to be perpendicular to the $C_{18}Fc$ monolayer is the key feature of the experiment.

The perpendicular orientation of the microelectrode to the air/water interface is accomplished by creating a sharp gradient of wettability along a single line on a gold surface. The key elements of the microelectrode design and its positioning at the air/water interface are shown in Figure 1. The microelectrodes are fabricated by vapor deposition of narrow strips of gold onto glass slides (see Experimental Section). Subsequently, all gold and glass surfaces were rendered hydrophobic by self-assembly of a long hydrocarbon chain monolayer. Prior to an electrochemical experiment, a gold-coated substrate is fractured in half, along a line perpendicular to the gold strip. This produces two microband electrodes with freshly exposed microbands of gold at the edge of each half of the glass slide. One microband electrode is then positioned at the air/water interface with the freshly created edge now in contact with water as shown in Figure 1. The high gradient of wettability between the clean, hydrophilic gold of the microband and the monolayer-coated, hydrophobic gold surface defines, along a single line, the coexistence front of three phases. It is this line that plays a role of a 1D electrode addressing a monolayer at the air/water interface. The reduction of dimensionality in this 2D electrochemical experiment does not affect the shape of the current voltage curves, as we demonstrate below.

Electrochemical methods have been used previously in the investigations of monolayers at the air/water interface.[5] However, the method described here is unique in that it directly probes the dynamics of the *lateral* diffusion processes in monolayers at the water surface. To this extent, our method parallels fluorescence microphotolysis (fluorescence recovery after photobleaching), which has been used extensively in the investigations of lateral

(1) Cadenhead, D. A. In *Structure and Properties of Cell Membranes*; Benga, G., Ed.; CRC Press: Boca Raton, FL, 1985; Vol. 3, p 21.
(2) Bard, A. J.; Faulkner, L. R. *Electrochemical Methods. Fundamentals and Applications*; Wiley: New York, 1980; Chapter 1.
(3) (a) Miller, C. J.; Widrig, C. A.; Charych, D. H.; Majda, M. *J. Phys. Chem.* **1988**, *92*, 1928. (b) Goss, C. A.; Miller, C. J.; Majda, M. *J. Phys. Chem.* **1988**, *92*, 1937. (c) Miller, C. J.; Majda, M. *Anal. Chem.* **1988**, *60*, 1168. (d) Bourdillon, C.; Majda, M. *J. Am. Chem. Soc.* **1990**, *112*, 1795.
(4) Goss, C. A.; Majda, M. *J. Electroanal. Chem.* **1991**, *300*, 377.
(5) (a) Fujihira, M.; Araki, T. *Chem. Lett.* **1986**, 921. (b) Zhang, X.; Bard, A. J. *J. Am. Chem. Soc.* **1989**, *111*, 8098.

0002-7863/91/1513-3340$02.50/0